Fundamental effects in nanoscale thermocapillary flow

Sung Hun Jin, Jizhou Song, Ha Uk Chung, Chenxi Zhang, Simon N. Dunham, Xu Xie, Frank Du, Tae-il Kim, Jong-Ho Lee, Yonggang Huang, and John A. Rogers

Citation: Journal of Applied Physics **115**, 054315 (2014); doi: 10.1063/1.4864487
View online: http://dx.doi.org/10.1063/1.4864487
View Table of Contents: http://scitation.aip.org/content/aip/journal/jap/115/5?ver=pdfcov
Published by the AIP Publishing

Fundamental effects in nanoscale thermocapillary flow

Sung Hun Jin,[1] Jizhou Song,[2,3] Ha Uk Chung,[4] Chenxi Zhang,[3] Simon N. Dunham,[5] Xu Xie,[4] Frank Du,[4] Tae-il Kim,[6,7] Jong-Ho Lee,[1] Yonggang Huang,[8] and John A. Rogers[4,a)]

[1]*School of Electrical Engineering and Computer Science (EECS) and the Inter-university Semiconductor Research Center (ISRC), Seoul National University, Seoul 151-742, Korea*
[2]*Department of Engineering Mechanics and Soft Matter Research Center, Zhejiang University, Hangzhou 310027, China*
[3]*Department of Mechanical and Aerospace Engineering, University of Miami, Coral Gables, Florida 33146, USA*
[4]*Department of Materials Science and Engineering, Frederick Seitz Materials Research Laboratory, University of Illinois at Urbana-Champaign, Urbana, Illinois 61801, USA*
[5]*Department of Chemistry and Biochemistry, Georgia Institute of Technology, Atlanta, Georgia 0332, USA*
[6]*School of Chemical Engineering, Sungkyunkwan University (SKKU), Suwon 440-746, Korea*
[7]*Center for Neuroscience Imaging Research (CNIR), Institute of Basic Science (IBS), Deajeon 308-811, Korea*
[8]*Departments of Civil and Environmental Engineering, and Mechanical Engineering, Center for Engineering and Health, and Skin Disease Research Center, Northwestern University, Evanston, Illinois 60208, USA*

(Received 12 January 2014; accepted 25 January 2014; published online 7 February 2014)

When implemented on the nanoscale, material flows driven by gradients in temperature, sometimes known as thermocapillary flows, can be exploited for various purposes, including nanopatterning, device fabrication, and purification of arrays of single walled carbon nanotubes (SWNTs). Systematic experimental and theoretical studies on thermocapillary flow in thin polymer films driven by heating in individual metallic SWNT over a range of conditions and molecular weights reveal the underlying physics of this process. The findings suggest that the zero-shear viscosity is a critical parameter that dominates the dependence on substrate temperature and heating power. The experimentally validated analytical models in this study allow assessment of sensitivity to other parameters, such as the temperature coefficient of surface tension, the thermal interface conductance, and the characteristic length scale of the heated zone. © *2014 AIP Publishing LLC*. [http://dx.doi.org/10.1063/1.4864487]

Recent reports highlight the ability to use nanoscale, thermally driven processes of pattern formation for applications in ultralow power phase-change memory,[1] nanolithography,[2–4] purification of aligned arrays single walled carbon nanotubes (SWNTs),[5] and others. In these examples, self-aligned structures in thin film coatings form as a result of local increases in temperature induced at the positions of Si or metal nanowires[2–4] or metallic SWNTs (m-SWNTs).[1,5] Some of these phenomena are reported to involve physical evaporation and/or chemical change in the films. In one case, data indicate a process of physical mass transport, or flow, that depends on temperature, gradients in temperature, and physical/chemical properties of the film and substrate support. Such flows can occur in organic small molecule or polymer films at peak temperatures of just a few degrees, for sources of heat that have nanoscale dimensions. In one application, films coated onto aligned arrays of SWNTs undergo flow only at regions of selective current injection, and Joule heating, at the m-SWNT. This process creates openings that allow removal of the m-SWNTs by gas phase etching, in a manner that leaves the semiconducting SWNTs unaltered. A full understanding of this process is necessary for further optimization and use of this physics not only in purification of SWNT arrays but in nanolithography, device fabrication, and other areas as well. Here, we report systematic experimental and theoretical studies that highlight, directly and indirectly, the essential aspects of nanoscale thermocapillary flows in films of polystyrene (PS), driven by Joule heating[1,5] in individual SWNTs. Quantitative agreement between experiment and theory establishes use of the models reported here for predictive assessment of the thermocapillary flow process. One key conclusion is that the viscosity[6,7] is a critical parameter that largely defines the influence of substrate temperature and rates of Joule heating on this process.

Fig. 1(a) provides a scanning electron microscope (SEM) image of an individual SWNT with a pair of metal electrode contacts. For studies reported here, ST-quartz wafers serve as substrates, with Ti/Pd (=2/40 nm) as contacts, separated by 30 μm.[5,8] For such devices formed with m-SWNTs, the voltage drops primarily along the length of the m-SWNTs, rather than at the contacts.[8] Spin casting thin films of PS on top of such devices and then applying a DC bias across the electrodes initiates nanoscale thermocapillary flow along the length of the heated m-SWNT, driven by the temperature dependent surface tension in the film, as described subsequently. Fig. 1(b) shows a typical trench that forms as a result. The trench width (W_{Tc}) is defined as the distance between the ridges that form in the PS on either side of the m-SWNT.[5] Studies involve PS (Sigma Aldrich, Inc) with M_w between 2.5 kg/mol to 30 kg/mol, dissolved in toluene to from a 0.8 wt. % solution that is passed through a PVDF (polyvinylidene fluoride) membrane filter with nominal pore size of 0.2 μm (Whatman^{TM}) to remove any particulates or polymer aggregates. Typical film

a)Author to whom correspondence should be addressed. E-mail: jrogers@illinois.edu.

thicknesses are $t_{PS} = 30\,\text{nm} \pm 3\,\text{nm}$. Thermocapillary flow occurs on a temperature-controlled substrate ($T_o = 353\,\text{K}$) in a vacuum chamber (Lake Shore Cryotronics, Inc.) at a base pressure of $\sim 1\times10^{-4}$ Torr. The process involves applying a DC bias for 10 min while monitoring the current with a parameter analyzer (Agilent 4155 C). An atomic force microscope (AFM; Asylum MFP 3D, tapping mode) yields images of the patterns of PS induced by thermocapillary flow. Soaking the sample in toluene, drying under a stream of nitrogen, and then baking on a hotplate (110 °C for 10 min) allows its re-use in multiple experiments.

Fig. 1(c) shows a collection of AFM images of trenches that form under identical overall conditions (i.e., average power dissipation per unit length of the SWNT, $Q_0 \sim 30\,\mu\text{W}/\mu\text{m}$, substrate temperature $T_o = 353\,\text{K}$, and base pressure $\sim 1\times10^{-4}$ Torr for 10 min) using PS with M_w from 17.5 kg/mol to 2.5 kg/mol. The results indicate that W_{Tc} increases significantly with decreasing M_w, as summarized by the red symbols in Fig. 1(d). The physics of this process is essentially unidirectional, such that the evolution of film thickness $h(x,t)$ can be approximated by the one dimensional lubrication equation[5]

$$\frac{\partial h}{\partial t} + \frac{\partial}{\partial x}\left[\frac{\tau h^2}{2\eta} + \frac{h^3}{3\eta}\frac{\partial}{\partial x}\left(\gamma\frac{\partial^2 h}{\partial x^2}\right)\right] = 0 \qquad (1)$$

with the initial condition $h(x, t=0) = h_0$, where h_0 is the initial film thickness, and the boundary conditions $h(x = \pm\infty, t) = h_0$ and $\partial^2 h/\partial x^2 (x = \pm\infty, t) = 0$ (zero pressure). Here, γ is the surface tension, which usually depends linearly on the temperature T [i.e., $\gamma = \gamma_0 - \gamma_1(T - 273)$] where γ_0 is the surface tension at 273 K and γ_1 is the temperature coefficient of the surface tension, $\tau = \frac{\partial \gamma}{\partial T}\frac{\partial T}{\partial x}$ is the thermocapillary stress, and η is the film viscosity. For polystyrene, γ_0 and γ_1 are taken as 47.4×10^{-3} N/m and 0.078×10^{-3} N/(mK),[9] respectively, for all PS materials examined since γ_0 and γ_1 depend only slightly on M_w (less than 5% change for γ_0 and 20% change for γ_1 with M_w between 2 kg/mol to 30 kg/mol).[9] The model suggests that low viscosity facilitates physical mass transport induced by spatial variations in surface tension due to temperature gradients created by Joule heating in the m-SWNT. The zero-shear viscosity, η, can be connected to M_w via the Vogel equation,[7] $\eta = Ae^{\frac{B}{\alpha_f(T-T_\infty)}}$, where A is the structure factor, B/α_f is a constant,[7] and T_∞ is the Vogel temperature, respectively. Literature[7] suggests that $B/\alpha_f \sim (1620 \pm 50)$ K, $A = 1.925\times10^{-8} M_w^{1.25}$ Pa · s, and $T_\infty = 321.4 - 8.3\times10^4 M_w^{-1}$ K, both with M_w in g/mol. We use $B/\alpha_f = 1640$ K, chosen within the range defined by the literature, but with a specific value that leads to agreement between experiment and theory for the trench width ($\sim 0.62\,\mu$m) at $T_0 = 353\,\text{K}$, $Q_0 = 30\,\mu\text{W}/\mu\text{m}$ and $M_w = 2.5$ kg/mol after 10 min of heating. Calculated viscosities from the Vogel equation appear as blue symbols in Fig. 1(d).

The temperature distribution for Eq. (1) can be approximated by the surface temperature[5] of the film calculated as a result of heating of the m-SWNT, which can be written

$$T(x) = \frac{1}{k_f \pi}\int_{-L/2}^{L/2} du \int_0^\infty \frac{Q_0 e^{-\xi h_0}\left(1 + \frac{k_s\xi}{\zeta}\right) J_0\left(\xi\sqrt{u^2 + x^2}\right)}{-\left(1 + \frac{k_s\xi}{\zeta} - \frac{k_s}{k_f}\right)e^{-2\xi h_0} + \left(1 + \frac{k_s\xi}{\zeta} + \frac{k_s}{k_f}\right)} d\xi + T_0, \qquad (2)$$

where k_s and k_f are the thermal conductivity of PS and quartz, respectively, L is the length of the SWNT, ζ is the interface thermal conductance between PS and quartz, and J_0 is the 0th order Bessel function of the first kind. Here, $h_0 = 30$ nm, $k_f = 0.15\,\text{Wm}^{-1}\text{K}^{-1}$ (Ref. 10), and $k_s = 6\,\text{Wm}^{-1}\text{K}^{-1}$ (Ref. 11). Compared with that for the case of $\zeta = \infty$, the computed peak temperatures at the surface of the PS are only ~35% higher for $\zeta = 10^8\,\text{W}/(\text{m}^2\text{K})$ and ~5% higher for $10^9\,\text{W}/(\text{m}^2\text{K})$, which are sufficiently small that they do not affect any of the major conclusions associated with this study. Therefore, all calculations in this paper correspond to the temperature computed with $\zeta = \infty$, i.e.,

$$T(x) = \frac{1}{2k_s\pi}\int_{-\frac{L}{2}}^{\frac{L}{2}} du \int_0^\infty \frac{Q_0 J_0\left(\xi\sqrt{u^2 + x^2}\right)}{\cosh(\xi h_0) + \frac{k_f}{k_s}\sinh(\xi h_0)} d\xi + T_0. \qquad (3)$$

Equation (1) is equivalent to a pair of coupled partial differential equations $\frac{\partial h_1}{\partial t} = \frac{\partial}{\partial x}\left(-\frac{\tau h_1^2}{2\eta} - \frac{h_1^3}{3\eta}\frac{\partial \gamma}{\partial x}h_2 - \frac{h_1^3\gamma}{3\eta}\frac{\partial h_2}{\partial x}\right)$ and $\frac{\partial^2 h_1}{\partial x^2} - h_2 = 0$ with $h_1 = h$, initial conditions $h_1(x, t=0) = h_0$ and $h_2(x, t=0) = 0$, and boundary conditions $h_1(x = \pm\infty, t) = h_0$ and $h_2(x = \pm\infty, t) = 0$. The Fortran solver PDE_1D_MG can be used to evaluate these equations (i.e., h_1 and h_2), to yield the evolution of the film thickness $h(x,t)$. The dashed line in Fig. 1(d) shows the computed value of W_{Tc} for parameters equivalent to experiment: 10 min of heating at $T_0 = 353\,\text{K}$ and $Q_0 = 30\,\mu\text{W}/\mu\text{m}$. The results agree remarkably well with experiment. The scaling trends arise mainly from variations in A, which yields a power law dependence of η on M_w ($\propto M_w^{1.25}$).[7]

The values of T_0 and Q_0 are also important. Fig. 2(a) shows AFM images of results of thermocapillary flow in PS with $M_w = 2.5$ kg/mol and $Q_0 = 30\,\mu\text{W}/\mu\text{m}$ for 10 min, with T_0 between 313 K to 353 K. The findings indicate that W_{Tc} increases dramatically with increases in T_0. Fig. 2(b) shows

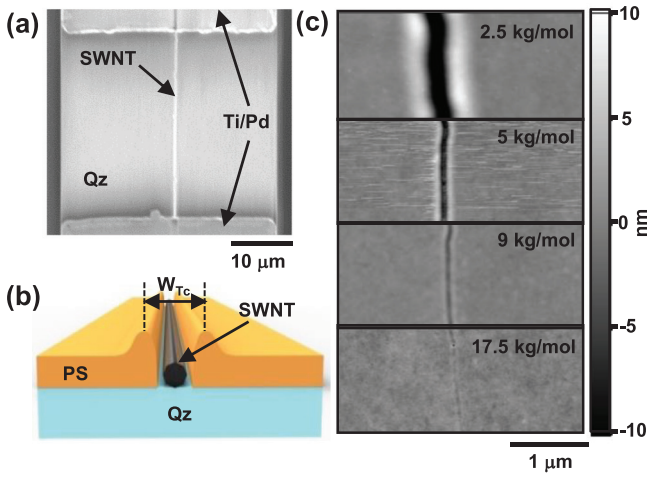

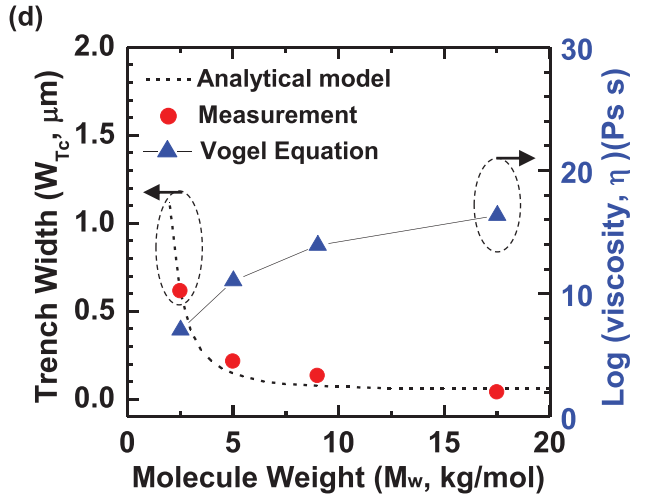

FIG. 1. (a) SEM image of an individual metallic SWNT with a pair of electrode contacts of Ti/Pd on a quartz (Qz) substrate, (b) schematic illustration showing the SWNT (grey), the Qz substrate (blue), and a layer of PS (gold) after nanoscale thermocapillary flow induced by Joule heating in the SWNT. The parameter W_{Tc} defines the width of the trench that forms. (c) AFM images of films of PS with molecule weights (M_w) ranging from 2.5 kg/mol to 17.5 kg/mol after inducing nanoscale thermocapillary flows by Joule heating in an underlying SWNT (power dissipation $Q_0 \sim 30$ μW/μm) at a substrate temperature, $T_0 = 353$ K. (d) Dependence of W_{Tc} on M_w of PS (red circles). Also plotted is the zero-shear viscosity, η of PS determined by the Vogel equation (blue triangles). The dashed line corresponds to W_{Tc} computed using an analytical model for nanoscale thermocapillary flow.

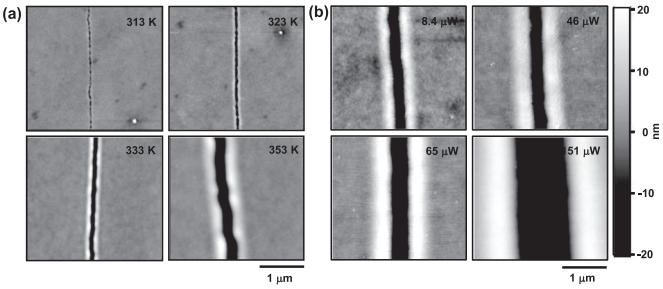

FIG. 2. (a) AFM images after nanoscale thermocapillary flow in a film of PS ($M_w = 2.5$ kg/mol) induced by Joule heating of an underlying SWNT at a power per unit length of 30 μW/μm, for substrate temperatures between 313 K to 353 K. (b) AFM images after nanoscale thermocapillary flow in a film of PS ($M_w = 2.5$ kg/mol) induced by Joule heating of an underlying SWNT at powers per unit length of between 8.4 μW/μm to 214 μW/μm, at a substrate temperature (353 K).

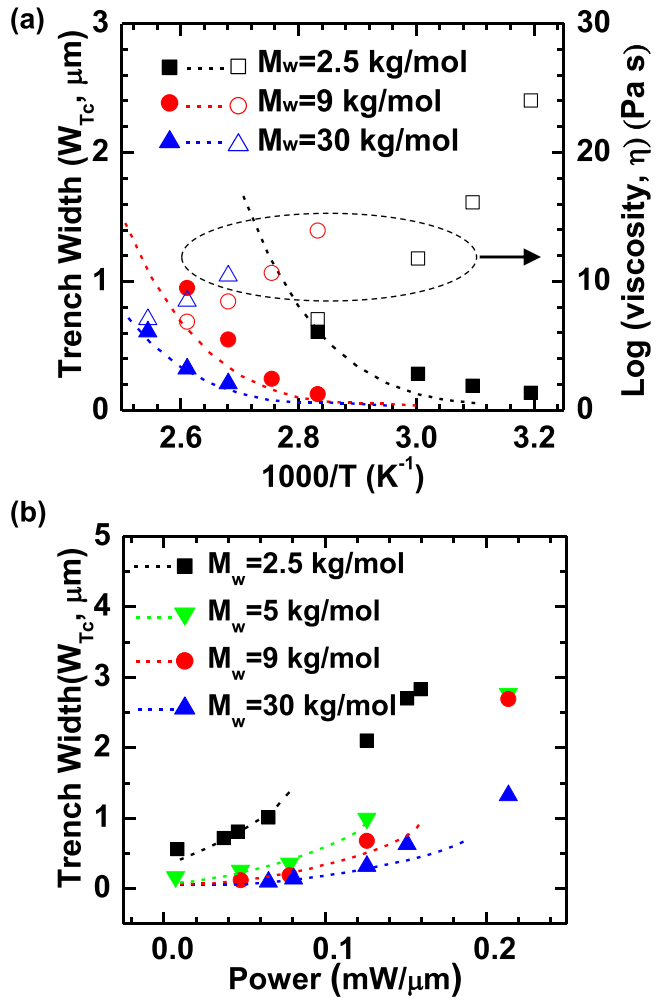

FIG. 3. (a) Trench width (W_{Tc}) and zero-shear viscosity (η) of polystyrene as a function of substrate temperature (T_0) between 313 K to 393 K, for PS films with different M_w (2.5, 9, and 30 kg/mol). The solid symbols and dashed lines correspond to measured and computed values for W_{Tc}. The open symbols correspond to values of η computed using the Vogel equation. (b) W_{Tc} as a function of power per unit length dissipated in the SWNT (Q_0) from 8.4 μW/μm to 214 μW/μm for PS films with different M_w (2.5, 5, 9, and 30 kg/mol). The solid symbols and dashed lines correspond to measured and computed values for W_{Tc}.

effects of changing Q_0 from 8.4 to 151 μW/μm for $T_0 = 353$ K and PS with $M_w = 2.5$ kg/mol at $T_0 = 353$ K. Clearly, as with T_0, W_{Tc} depends strongly on Q_0. Fig. 3(a) summarizes a set of results similar to those of Fig. 2(a). The Arrhenius type scaling arises from the temperature dependence of η, as confirmed from results computed with Eqs. (1) and (2). Likewise, Fig. 3(b) shows a collection of measurements like those of Fig. 2(b), which reveal scaling with Q_0. The trench width is captured with the analytical solution without any fitting, thereby providing further indication that η is, to within experimental uncertainties, entirely responsible for the observed variations. We note that the calculations cease to be valid above a critical value $h(x=0,t)=0$.

In summary, the results presented here indicate that effects of temperature, power dissipation, and molecular weight on nanoscale thermocapillary flow all arise primarily from associated variations in viscosity. The sensitivity to the temperature coefficient of surface tension (γ_1), the thermal interface conductance (ζ) are comparatively small, for values of these parameters that lie within ranges reported in the literature.[7,9] For the conditions examined here, the maximum temperature gradient $(dT/dx)_{max}$, for a given Q_0, shows little dependence on the width of the heat source for values ranging from those corresponding to a SWNT (i.e., $\sim$1 nm) to $\sim$100 nm diameter range; at 1 μm, the gradient is reduced by nearly an order of magnitude. These and other insights can be developed from an examination of the physics implied by the experimentally validated models reported here. In particular, engineering design rules for control of flows associated with this type of thermally induced pattern formation can be defined. The immediate relevance is to recently described, low temperature approaches for purifying arrays of SWNTs, but can be extended to other areas in nanopatterning and device fabrication where such effects could be useful.

J.S. acknowledges the supports from the Thousand Young Talents Program of China and NSFC (Grant No. 11372272).

[1]F. Xiong, M.-H. Bae, Y. Dai, A. D. Liao, A. Behnam, E. A. Carrion, S. Hong, D. Ielmini, and E. Pop, Nano Lett. **13**, 464 (2013).
[2]I. Park, Z. Li, A. P. Pisano, and R. S. Williams, Nano Lett. **7**, 3106 (2007).
[3]H. Zhang, C.-L Wong, Y. Hao, R. Wang, X. Liu, F. Stellacci, and J. T. L. Thong, Nanoscale **2**, 2302 (2010).
[4]C. Y. Jin, Z. Li, R. S. Williams, K.-C. Lee, and I. Park, Nano Lett. **11**, 4818 (2011).
[5]S. H. Jin, S. N. Dunham, J. Song, X. Xie, J. Kim, C. Lu, A. Islam, F. Du, J. Kim, J. Felts, Y. Li, F. Xiong, M. A. Wahab, M. Menon, E. Cho, K. L. Gross, D. J. Lee, H. U. Chung, E. Pop, M. A. Alam, W. P. King, Y. Huang, and J. A. Rogers, Nat. Nanotechnol. **8**, 347 (2013).
[6]G. B. McKenna, G. Hadziioannou, P. Lutz, G. Hild, C. Strazielle, C. Straupe, P. Rempp, and A. J. Kovacs, Macromolecules **20**, 498 (1987).
[7]J.-C. Majeste, J.-P. Montfort, A. Allal, and G. Marin, Rheol Acta **37**, 486 (1998).
[8]M. A. Wahab, S. H. Jin, A. E. Islam, J. Kim, J. Kim, W.-H. Yeo, D. J. Lee, H. U. hung, J. A. Rogers, and M. A. Alam, ACS Nano **7**, 1299 (2013).
[9]J. C. Moreira and N. R. Demarquette, J. Appl. Polym. Sci. **82**, 1907 (2001).
[10]P. Ferkl, R. Pokorny, M. Bobak, and J. Kosek, Chem. Eng. Sci. **97**, 50 (2013).
[11]A. E. Beck, D. M. Darbha, and H. H. Schloessin, Phys. Earth Planet. Interiors **17**, 35 (1978).